High-Energy Behavior near Threshold: Massive Quantum Electrodynamics*

HUNG CHENG†
Department of Mathematics, Massachusetts Institute of Technology, Cambridge, Massachusetts 02139
AND
TAI TSUN WU
Gordon McKay Laboratory, Harvard University, Cambridge, Massachusetts 02138
(Received 20 April 1970)

In this paper we study all scattering amplitudes in quantum electrodynamics in the limit $s\to\infty$, with t near or at the two-photon threshold. In this limit, the power of s for a diffractive amplitude with a two-photon cut is found to be promoted from 1 to $\frac{3}{2}$. The fourth-order electron-electron scattering amplitude is first studied by the method of Feynman parameters. The method of impact diagrams is next generalized to handle the more complicated cases. We then apply the new method explicitly to the lowest-order diffractive amplitude for electron-electron scattering, Compton scattering, and photon-photon scattering. A general case $a+b\to a'+b'$ is also discussed. We find that the scattering amplitude is now factorized and the existence of a Regge pole is suggested. This is then verified by a study of the tower diagrams. Thus the leading singularity in the J plane, while being a pair of branch points for $t\leq 0$, is a moving Regge pole located to the right of $J=\frac{3}{2}$ as t is near $4\lambda^2$. The Gribov paradox is thereby automatically resolved.

1. INTRODUCTION

OVER the past two years, we have made a field-theoretic study of high-energy diffractive scattering near the forward direction.[1–7] For a two-body scattering process $a+b\to c+d$, the region we concentrated on is $s\to\infty$, with t fixed at a nonpositive value, where s is the square of the c.m. energy and t is the negative of the momentum transfer squared. In this paper, we shall consider scattering amplitudes in quantum electrodynamics in the region $s\to\infty$, with t fixed at a positive value near $4\lambda^2$, where λ is the mass of the "photon." More precisely, $t-4\lambda^2$ will be taken to be of the order of s^{-1}. This is an unphysical region.

Our motivations for studying the present problem are as follows. Take, for example, the process of electron-electron scattering. In the limit $s\to\infty$, with $t\leq 0$, the second- and the fourth-order amplitudes, representing the one-photon and two-photon exchange processes, respectively, are proportional to s, and give naturally a constant value to the differential cross section $d\sigma/dt$. There is, in fact, a wide class of diagrams which yields amplitudes proportional to s. Physically, they give rise to the two-fireball picture in which each of the electrons and its created particles move together with approximately equal velocities, and the scattering proceeds through instantaneous exchanges of photons. There are, however, processes which cannot be described by this picture. These diagrams give amplitudes of the order of $s(\ln s)^n$, $n=1, 2, 3, \ldots$. The lowest-order diagrams which give uncanceled $s(\ln s)^n$ terms are the ones with n electron loops.[8] They are illustrated in Fig. 1, and their leading term has been explicitly evaluated.[8] Physically, the existence of logarithmic factors is due to the contribution of the slowly moving particles created, and is directly related to the phenomenon of pionization.[9] If we add up these leading terms over all n, we obtain an amplitude of the order of $s^{1+11\alpha^2\pi/32}(\ln s)^{-2}$ at $t=0$, where α is the fine-structure constant. This amplitude exceeds the unitarity limit, and therefore cannot be the correct asymptotic form of the electron-electron scattering amplitude. Now a perturbation series can always be made to satisfy unitarity by including more diagrams. In the present case, we may unitarize the amplitudes from the diagrams of Fig. 1 by adding the amplitudes from the diagrams of Fig. 2, as the latter also have terms of the order of $s(\ln s)^n$, $n=1, 2, 3, \ldots$. The sum of all these amplitudes does not violate unitarity. This means that for $t\leq 0$, the diagrams in Fig. 2 cannot be neglected. We must note, however, that satisfying the unitarity condition is no guarantee for the answer to be correct, and the precise asymptotic amplitude for a high-energy diffractive process is still to be found.

The situation is somewhat simpler in the unphysical region $s\to\infty$, $t\sim 4\lambda^2$. We note that the point $t=4\lambda^2$ is a branch point for the amplitudes of Fig. 1. In fact, as $t\to 4\lambda^2$, the high-energy amplitude for the n-loop diagrams increases dramatically, not so much by some factor of $\ln s$, but rather by a power of s. Specifically, at $t=4\lambda^2$, the high-energy amplitude for the n-loop diagrams of Fig. 1 is "promoted" from $s(\ln s)^n$ to $s^{3/2}(\ln s)^n$. As the amplitudes in Fig. 2 remain to be of the same order of magnitude and are therefore negligible, it becomes reasonable to expect that summing leading terms gives the correct answer at $t=4\lambda^2$.

* Work supported in part by the U. S. Atomic Energy Commission under Contract No. AT(30-1)-4101.
† Work supported in part by the National Science Foundation under Grant No. GP-13775.

[1] H. Cheng and T. T. Wu, Phys. Rev. Letters **22**, 666 (1969).
[2] H. Cheng and T. T. Wu, Phys. Rev. **182**, 1852 (1969).
[3] H. Cheng and T. T. Wu, Phys. Rev. **182**, 1868 (1969).
[4] H. Cheng and T. T. Wu, Phys. Rev. **182**, 1873 (1969).
[5] H. Cheng and T. T. Wu, Phys. Rev. **182**, 1899 (1969).
[6] H. Cheng and T. T. Wu, Phys. Rev. D **1**, 1069 (1970).
[7] H. Cheng and T. T. Wu, Phys. Rev. D **1**, 1083 (1970).
[8] H. Cheng and T. T. Wu, Phys. Rev. D **1**, 2775 (1970).
[9] H. Cheng and T. T. Wu, Phys. Rev. Letters **23**, 1311 (1969).

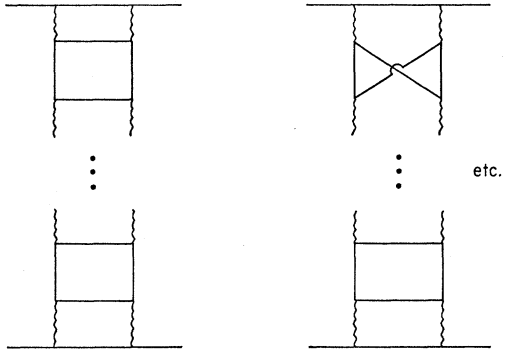

FIG. 1. Tower diagrams for electron-electron scattering. The s channel is from left to right and the t channel is from bottom to top.

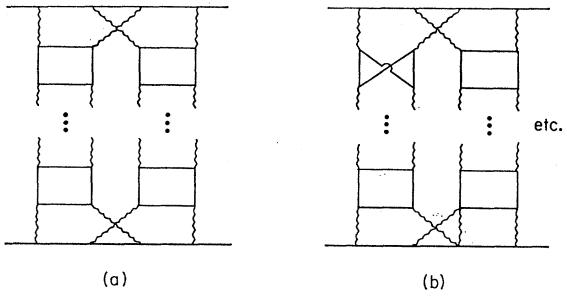

FIG. 2. Diagrams which unitarize the diagrams in Fig. 1.

The phenomenon of "promotion" is not entirely unfamiliar. In potential scattering, for example, it is known that, if the potential is small and attractive, the leading Regge pole is near $l=-1$ when the energy is away from the threshold, but is at the right of $l=-\frac{1}{2}$ at the threshold.[10] A similar phenomenon occurs in φ^3 theory. This will be discussed in some detail in the two following papers.[11,12]

The contents of this paper are as follows. In Sec. 2, we calculate the fourth-order amplitude for electron-electron scattering in the limit $s\to\infty$, with $t=4\lambda^2+O(s^{-1})$. This is accomplished via Feynman parameters. The method of Feynman parametrization is not convenient when the order is high, and in Sec. 3 we generalize the impact-diagram method for this purpose. In Sec. 4 we apply the new method to various scattering problems. In Sec. 5 we apply this method to the tower diagrams of Fig. 1. Finally, in Sec. 6 we discuss the physical significance of our results. A summary of this and the two following papers can be found elsewhere.[13]

2. FOURTH-ORDER ELECTRON-ELECTRON SCATTERING

We begin the investigation of threshold behavior in quantum electrodynamics with the simplest nontrivial case, namely, fourth-order electron-electron scattering as shown in Fig. 3. Let λ be the mass of the photon, assumed to be nonzero throughout this paper; then the total contribution of these two diagrams is[14,3]

$$\mathfrak{M}_1^{(--)}=\mathfrak{M}_{11}+\mathfrak{M}_{12}, \tag{2.1}$$

where

$$\mathfrak{M}_{11}=-ie^4(2\pi)^{-4}\int d^4q\,\frac{[\bar u(p_2)\gamma_\nu(-\boldsymbol{q}+\boldsymbol{r}_2+m)\gamma_\mu u(p_1)][\bar u(p_2')\gamma_\mu(\boldsymbol{q}+\boldsymbol{r}_3+m)\gamma_\nu u(p_1')]}{[(r_2-q)^2-m^2+i\epsilon][(r_1+q)^2-\lambda^2+i\epsilon][(r_3+q)^2-m^2+i\epsilon][(r_1-q)^2-\lambda^2+i\epsilon]} \tag{2.2}$$

and

$$\mathfrak{M}_{12}=-ie^4(2\pi)^{-4}\int d^4q\,\frac{[\bar u(p_2)\gamma_\nu(-\boldsymbol{q}+\boldsymbol{r}_2+m)\gamma_\mu u(p_1)][\bar u(p_2')\gamma_\mu(-\boldsymbol{q}+\boldsymbol{r}_3+m)\gamma_\nu u(p_1')]}{[(r_2-q)^2-m^2+i\epsilon][(r_1+q)^2-\lambda^2+i\epsilon][(r_3-q)^2-m^2+i\epsilon][(r_1-q)^2-\lambda^2+i\epsilon]}. \tag{2.3}$$

Since the metric used here is $(1,-1,-1,-1)$,

$$t=(p_1-p_2)^2=(p_1'-p_2')^2$$

is nonpositive in the physical region. In obtaining the asymptotic behavior as $s\to\infty$ with $t\leq 0$, the numerator is first simplified.[3] This simplification holds for all t. By (2.11) and (2.18) of Ref. 3, (2.2) and (2.3) reduce, for $j=1$, to

$$\mathfrak{M}_{1j}\sim e^4(4\pi)^{-2}s^2m^{-2}\delta_{12}\delta_{1'2'}\int_0^1 d\alpha_1d\alpha_2d\alpha_3d\alpha_4\,\frac{(1-\alpha_1)(1-\alpha_3)\delta(1-\alpha_1-\alpha_2-\alpha_3-\alpha_4)}{[-(-1)^j\alpha_1\alpha_3s+\alpha_2\alpha_4t-(\alpha_1+\alpha_3)^2m^2-(\alpha_2+\alpha_4)\lambda^2+i\epsilon]^2} \tag{2.4}$$

for $s\to\infty$. It is thus observed that the presence of numerator factors has mainly the effect of multiplication by s^2, and otherwise does not affect the threshold behavior.

Consider first the case where t is at the two-photon

[10] R. G. Newton, J. Math. Phys. **3**, 867 (1962).
[11] H. Cheng and T. T. Wu, first following paper, Phys. Rev. D **2**, 2285 (1970).
[12] H. Cheng and T. T. Wu, second following paper, Phys. Rev. D **2**, 2298 (1970).
[13] H. Cheng and T. T. Wu, Phys. Rev. Letters **24**, 759 (1970).
[14] The terms $\mathfrak{M}_{11}$ and $\mathfrak{M}_{12}$ correspond, respectively, to $\mathfrak{M}_1$ and $\mathfrak{M}_2$ of Ref. 3. Otherwise the notations here are the same as those of Ref. 3.

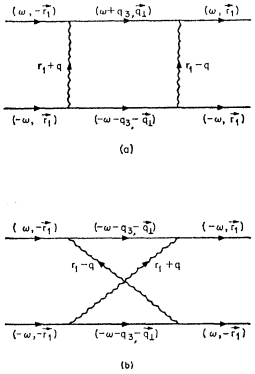

FIG. 3. Lowest-order diagrams for electron-electron scattering with a two-photon cut in the t channel.

threshold. More precisely, we want to study the behavior of $\mathfrak{M}_{11}$ and $\mathfrak{M}_{12}$ as $s\to\infty$ with $t=4\lambda^2$. Let

$$\alpha_1=\alpha_1'\lambda^2/s,\quad \alpha_3=\alpha_3'\lambda^2/s,$$

and

$$\alpha_2=\tfrac{1}{2}(1+\lambda x/\sqrt{s}); \tag{2.5}$$

then

$$\alpha_4\sim\tfrac{1}{2}(1-\lambda x/\sqrt{s}) \tag{2.6}$$

and

$$\mathfrak{M}_{1j}\sim e^4(4\pi)^{-2}\lambda^{-3}s^{3/2}m^{-2}\delta_{12}\delta_{1'2'}\int_0^\infty d\alpha_1'd\alpha_3'dx$$
$$\times[-(-1)^j\alpha_1'\alpha_3'-(\alpha_1'+\alpha_3'+x^2)+i\epsilon]^{-2}. \tag{2.7}$$

Explicit integration then gives that, for large s with $t=4\lambda^2$,

$$\mathfrak{M}_{11}\sim\tfrac{1}{32}e^4i\lambda^{-3}m^{-2}s^{3/2}\delta_{12}\delta_{1'2'},$$
$$\mathfrak{M}_{12}\sim\tfrac{1}{32}e^4\lambda^{-3}m^{-2}s^{3/2}\delta_{12}\delta_{1'2'}, \tag{2.8}$$

and hence

$$\mathfrak{M}_1\sim\tfrac{1}{32}e^4(1+i)\lambda^{-3}m^{-2}s^{3/2}\delta_{12}\delta_{1'2'}. \tag{2.9}$$

Note that, for $t=4\lambda^2$, the asymptotic behavior of $\mathfrak{M}_{11}$ and $\mathfrak{M}_{12}$ differ by a factor i, and hence there is no cancellation when added together. This is in marked contrast with the corresponding situation for $t\neq4\lambda^2$, where the leading terms of $\mathfrak{M}_{11}$ and $\mathfrak{M}_{12}$ cancel each other (see Sec. 2 of Ref. 3).

The generalization to the case where $t-4\lambda^2$ is of the order s^{-1} is immediate. Let

$$t=4\lambda^2(1-\lambda^2T/s); \tag{2.10}$$

then, when $s\to\infty$ for fixed T,

$$\mathfrak{M}_{11}\sim e^4(16\pi)^{-1}\lambda^{-3}m^{-2}s^{3/2}\delta_{12}\delta_{1'2'}(T+1-i\epsilon)^{-1/2}$$
$$\times\{\tfrac{1}{2}i\pi-\ln[(T-i\epsilon)^{1/2}+(T+1-i\epsilon)^{1/2}]\},$$
$$\mathfrak{M}_{12}\sim e^4(16\pi)^{-1}\lambda^{-3}m^{-2}s^{3/2}\delta_{12}\delta_{1'2'}(T-1-i\epsilon)^{-1/2} \tag{2.11}$$
$$\times\ln[(T-i\epsilon)^{1/2}+(T-1-i\epsilon)^{1/2}],$$

and hence

$$\mathfrak{M}_1^{(--)}\sim e^4(16\pi)^{-1}\lambda^{-3}m^{-2}s^{3/2}\delta_{12}\delta_{1'2'}$$
$$\times\{\tfrac{1}{2}i\pi(T+1-i\epsilon)^{-1/2}-(T+1-i\epsilon)^{-1/2}$$
$$\times\ln[(T-i\epsilon)^{1/2}+(T+1-i\epsilon)^{1/2}]$$
$$+(T-1-i\epsilon)^{-1/2}$$
$$\times\ln[(T-i\epsilon)^{1/2}+(T-1-i\epsilon)^{1/2}]\}. \tag{2.12}$$

Equation (2.12) gives completely the asymptotic behavior of $\mathfrak{M}_1$ near the elastic threshold.

3. IMPACT DIAGRAMS NEAR THRESHOLD

The calculations performed in the preceding section are based on Feynman diagrams. Now we know that Feynman diagrams are not particularly convenient for calculations of high-energy processes. It is therefore desirable to generalize the method of impact diagrams to cover the unphysical case when T given by (2.10) is fixed and $s\to\infty$. This generalization will prove especially useful in handling higher-order diagrams in the later sections.

Since promotion occurs only to diagrams with two-particle cuts in the t channel, we shall concentrate on such diagrams. In particular, the notation of black dot in impact diagrams will not be used. For the same reasons as discussed in Ref. 6, we shall perform the calculations with pre-Feynman perturbation method. Consider, for example, the scattering process $a+b\to a'+b'$. We first draw a diagram for the process. This diagram is not a Feynman diagram, as time is always increasing from left to right. It is also different from an impact diagram as there are no black dots, and the interaction between a and b is mediated by the exchange of photons. The propagators for the two exchanged photons, with four-momenta r_1+q and r_1-q, respectively, are $[(r_1+q)^2-\lambda^2+i\epsilon]^{-1}$ and $[(r_1-q)^2-\lambda^2+i\epsilon]^{-1}$, respectively. Let us assume that the photon of momentum r_1+q is the first one to be exchanged. Then the energy propagator for particle a after this exchange is given by

$$E_a+(r_1+q)_0-E_n=\{[(\omega^2+\mathbf{r}_{1\perp}^2+M_a^2)^{1/2}+(r_1+q)_0]$$
$$-[\sum_i(\omega^2\beta^2+\mathbf{p}_{i\perp}^2+m_i^2)^{1/2}+(r_1+q)_3]\}^{-1}$$
$$\sim\{(2\mathbf{r}_{1\perp}^2+M_a^2+M_{a'}^2)(4\omega)^{-1}$$
$$-\sum_i(\mathbf{p}_{i\perp}^2+m_i^2)/(2\omega\beta_i)+q_-+i\epsilon\}^{-1}, \tag{3.1}$$

where

$$q_-=q_0-q_3. \tag{3.2}$$

In (3.1), ω and $\mathbf{r}_{1\perp}$ are, respectively, the longitudinal and transverse components of the spatial momentum of a, and i denotes a particle in the intermediate state n, i.e.,

$$\sum_i\beta_i=1, \tag{3.3}$$

$$\sum_i\mathbf{p}_{i\perp}=\mathbf{q}_\perp\sim0, \tag{3.4}$$

since, as we shall see, $\mathbf{q}_\perp$ is of the order of ω^{-1}. Note that we have made use of[15]

$$r_{10}-r_{13}=(4\omega)^{-1}(M_{a'}{}^2-M_a{}^2). \tag{3.5}$$

If the photon of momentum r_1-q is the first one to be exchanged, the corresponding energy propagator is equal to (3.1) with q_- replaced by $-q_-$. Adding up these two terms, we get

$$-\lambda^2\omega^{-1}A[\tfrac{1}{4}\lambda^4\omega^{-2}(A-i\epsilon)^2-q_-{}^2]^{-1}, \tag{3.6}$$

where

$$A=\lambda^{-2}[\sum_i(\mathbf{p}_{i\perp}{}^2+m_i{}^2)/\beta_i+\lambda^2-\tfrac{1}{2}(M_a{}^2+M_{a'}{}^2)]. \tag{3.7}$$

Similarly, from particle b we get a factor

$$-\lambda^2\omega^{-1}B[\tfrac{1}{4}\lambda^4\omega^{-2}(B-i\epsilon)^2-q_+{}^2]^{-1}, \tag{3.8}$$

where

$$q_+=q_0+q_3$$

and

$$B=\lambda^{-2}[\sum_j(\mathbf{p}_{j'\perp}{}^2+m_{j'}{}^2)/\beta_{j'}+\lambda^2-\tfrac{1}{2}(M_b{}^2+M_{b'}{}^2). \tag{3.9}$$

In (3.9), j' denotes a particle in the intermediate state after one of the photons is exchanged, i.e.,

$$\sum_i\beta_{j'}=1, \tag{3.10}$$

$$\sum_j\mathbf{p}_{j'\perp}\sim 0. \tag{3.11}$$

At this point it is probably desirable to compare the above equations with those based on impact diagrams. In the latter, Eqs. (3.6) and (3.7) are approximated by $-2\pi i\delta(q_-)$ and $-2\pi i\delta(q_+)$, respectively. These approximations fail at $t=4\lambda^2$, since the resulting scattering amplitude contains the integral $\int d\mathbf{q}_\perp[(\mathbf{r}_1+\mathbf{q}_\perp)^2+\lambda^2]^{-1}\times[(\mathbf{r}_1-\mathbf{q}_\perp)^2+\lambda^2]^{-1}$, which is divergent due to the integration region $q_1\sim 0$, $q_2\sim 0$, $q_1=O(q_2{}^2)$, where q_1 is the component of $\mathbf{q}_\perp$ in the direction of $\mathbf{r}_{1\perp}$, and q_2 that in the other transverse direction. Thus, the *only* modification of the impact-diagram rules needed is to recover the energy denominators (3.6) and (3.8), and integrate over d^4q. Since q is of order $O(\omega^{-1})$, we may neglect q as compared to unity everywhere. In particular, we may set $q=0$ in all factors in the scattering amplitude, excluding the factors (3.6), (3.8), and the two photon propagators. Thus, to obtain the high-energy amplitude with T fixed, we only need to make the following replacement after applying the impact-diagram rules:

$$\begin{aligned}&(2\pi)^{-2}\int d\mathbf{q}_\perp[(\mathbf{r}_1+\mathbf{q}_\perp)^2+\lambda^2]^{-1}\\&\times[(\mathbf{r}_1-\mathbf{q}_\perp)^2+\lambda^2]^{-1}\to-(2\pi)^{-4}\lambda^4\omega^{-2}AB\\&\times\int d\mathbf{q}_\perp dq_+dq_-[(r_1+q)^2-\lambda^2+i\epsilon]^{-1}\\&\times[(r_1-q)^2-\lambda^2+i\epsilon]^{-1}[\tfrac{1}{4}\lambda^2\omega^{-2}(A-i\epsilon)^2-q_-{}^2]^{-1}\\&\times[\tfrac{1}{4}\lambda^4\omega^{-2}(B-i\epsilon)^2-q_+{}^2]^{-1}\\&\qquad\sim-is^{1/2}\lambda^{-3}(AB)^{-1/2}I(T/AB),\end{aligned} \tag{3.12}$$

where

$$\begin{aligned}I(x)=(4\pi)^{-1}\{&\tfrac{1}{2}i\pi(x+1-i\epsilon)^{-1/2}-(x+1-i\epsilon)^{-1/2}\\&\times\ln[(x-i\epsilon)^{1/2}+(x+1-i\epsilon)^{1/2}]+(x-1-i\epsilon)^{-1/2}\\&\times\ln[(x-i\epsilon)^{1/2}+(x-1-i\epsilon)^{1/2}]\}.\end{aligned} \tag{3.13}$$

Note that

$$I(0)=\tfrac{1}{8}(1+i). \tag{3.14}$$

The derivation of (3.13) is presented in Appendix A. One point is worth mentioning: An inspection of the integrand in (3.12) shows that q_+, q_-, and $\mathbf{q}_\perp$ are all of the order of ω^{-1}.

4. APPLICATION TO LOWEST-ORDER DIAGRAMS

In this section we shall apply the method developed in the preceding section to the lowest-order amplitudes of (i) $e+e\to e+e$, (ii) $e+\gamma\to e+\gamma$, and (iii) $\gamma+\gamma\to\gamma+\gamma$, valid for $s\to\infty$ with T fixed.

A. Electron-Electron Scattering

The diagrams we shall consider are illustrated in Fig. 3, and the corresponding amplitude has been calculated in Sec. 4 with the help of Feynman parameters. We shall now do the calculation with the new method.

Applying the impact-diagram rules, we obtain this amplitude as

$$\mathfrak{M}_1{}^{(--)}\sim is(2\pi)^{-2}(g^e)^2\int d\mathbf{q}_\perp[(\mathbf{r}_1+\mathbf{q}_\perp)^2+\lambda^2]^{-1}\times[(\mathbf{r}_1-\mathbf{q}_\perp)^2+\lambda^2]^{-1}, \tag{4.1}$$

valid for $t\neq 4\lambda^2$. An inspection of Fig. 3 gives

$$A=B=1; \tag{4.2}$$

thus, when T is fixed and $s\to\infty$, (4.1) and (3.12) give

$$\mathfrak{M}_1{}^{(--)}\sim s^{3/2}\lambda^{-3}(g^e)^2I(T). \tag{4.3}$$

Equation (4.3) is precisely (2.12).

B. Compton Scattering

Next we consider the scattering of a photon from an electron. For simplicity, let us take the mass of the external photons to be zero, while that of the exchanged photons remains λ.[16] When t is away from $4\lambda^2$, the scattering amplitude for Compton scattering in the sixth order is given by

$$is(2\pi)^{-2}\int d\mathbf{q}_\perp[(\mathbf{r}_1+\mathbf{q}_\perp)^2+\lambda^2]^{-1}\times[(\mathbf{r}_1-\mathbf{q}_\perp)^2+\lambda^2]^{-1}g^eg^\gamma, \tag{4.4}$$

where g^γ is the photon impact factor given by (3.15) of Ref. 6. When T is fixed and $s\to\infty$, the sixth-order

[15] See, for instance, Eq. (2.11) in H. Cheng and T. T. Wu, Phys. Rev. D 1, 459 (1970).

[16] For the more general case in which the external photons also have mass, see Ref. 15.

Compton scattering process is represented pictorially by the diagrams in Fig. 4. An inspection of Fig. 4 gives

$$A=\lambda^{-2}(\mathbf{p}_\perp{}^2+m^2)\beta^{-1}(1-\beta)^{-1} \tag{4.5}$$

and

$$B=1. \tag{4.6}$$

Thus

$$\mathfrak{M}^{(c)}\sim s^{3/2}\lambda^{-3}J^{e\gamma}(T), \tag{4.7}$$

where

$$J^{e\gamma}(T)=-\tfrac{1}{2}(2\pi)^{-3}e^4g^e\int d\mathbf{p}_\perp\int_0^1 d\beta\, I(T/A)A^{-1/2}[(\mathbf{p}_\perp+\beta\mathbf{r}_1)^2+m^2]^{-1}$$
$$\times\left\{\frac{\beta\omega^{-1}\,\mathrm{Tr}[\gamma_i(-\not{p}_1+m)\gamma_j(\not{p}_2+2\not{r}_1+m)\gamma_0(\not{p}_2+m)]}{(\mathbf{p}_\perp-\beta\mathbf{r}_1)^2+m^2}\right.$$
$$\left.+\frac{\frac{1}{2}\omega^{-2}\,\mathrm{Tr}[\gamma_i(-\not{p}_1+m)\gamma_0(-\not{p}_1-\not{r}_1+m)\gamma_j(\not{p}_2+\not{r}_1+m)\gamma_0(\not{p}_2+m)]}{(\mathbf{p}_\perp+(1-\beta)\mathbf{r}_1)^2+m^2}\right\}, \tag{4.8}$$

with

$$\mathbf{r}_1{}^2=-\lambda^2, \tag{4.9}$$

$$\mathbf{p}_1=[\beta\omega,\mathbf{p}_\perp], \tag{4.10}$$

and

$$\mathbf{p}_2=[(1-\beta)\omega,\,-\mathbf{r}_1-\mathbf{p}_1]. \tag{4.11}$$

In (4.8), i and j denote the polarization of the incoming and the outgoing photons, respectively. Alternatively, (4.8) can be written as

$$J^{e\gamma}(T)=-\tfrac{1}{2}\pi^{-3}e^4g^e\int d\mathbf{p}_\perp\int_0^1 d\beta\, I(T\lambda^2\beta(1-\beta)(\mathbf{p}_\perp{}^2+m^2)^{-1})\lambda\beta^{1/2}(1-\beta)^{1/2}(\mathbf{p}_\perp{}^2+m^2)^{-1/2}[(\mathbf{p}_\perp+\beta\mathbf{r}_1)^2+m^2]^{-1}$$
$$\times\left\{\frac{\delta_{ij}\beta^2\mathbf{r}_1{}^2+2\beta(1-\beta)(p_{1i}p_{1j}-\beta^2r_{1i}r_{1j})}{(\mathbf{p}_\perp-\beta\mathbf{r}_1)^2+m^2}-\frac{\delta_{ij}(\tfrac{1}{2}-\beta)^2\mathbf{r}_1{}^2+2\beta(1-\beta)[(p_\perp+\frac{1}{2}r_1)_i(p_\perp+\frac{1}{2}r_1)_j-(\frac{1}{2}-\beta)^2r_{1i}r_{1j}]}{[\mathbf{p}_\perp+(1-\beta)\mathbf{r}_1]^2+m^2}\right\}, \tag{4.12}$$

with (4.9) understood.

C. Photon-Photon Scattering

When t is away from $4\lambda^2$, the scattering amplitude for photon-photon scattering in the eighth order is given by

$$is(2\pi)^{-2}\int d\mathbf{q}_\perp\,[(\mathbf{r}_1+\mathbf{q}_\perp)^2+\lambda^2]^{-1}[(\mathbf{r}_1-\mathbf{q}_\perp)^2+\lambda^2]^{-1}[\mathcal{G}^\gamma(\mathbf{r}_1,\mathbf{q}_\perp)]^2. \tag{4.13}$$

When T is fixed and $s\to\infty$, the eighth-order photon-photon scattering process is represented pictorially by the diagrams in Fig. 5. An inspection of Fig. 5 gives

$$A=\lambda^{-2}(\mathbf{p}_\perp{}^2+m^2)\beta^{-1}(1-\beta)^{-1}, \tag{4.14}$$

$$B=\lambda^{-2}(\mathbf{p}_\perp{}'^2+m^2)\beta'^{-1}(1-\beta')^{-1}. \tag{4.15}$$

Thus

$$\mathfrak{M}^{(\gamma\gamma)}\sim s^{3/2}\lambda^{-3}J^{\gamma\gamma}(T), \tag{4.16}$$

where

$$J^{\gamma\gamma}(T)=\tfrac{1}{4}\pi^{-6}e^8\int d\mathbf{p}_\perp d\mathbf{p}_\perp{}'\int_0^1 d\beta\int_0^1 d\beta'\, I(TA^{-1}B^{-1})(AB)^{-1/2}[(\mathbf{p}_\perp+\beta\mathbf{r}_1)^2+m^2]^{-1}[(\mathbf{p}_\perp{}'+\beta'\mathbf{r}_1)^2+m^2]^{-1}$$
$$\times\left\{\frac{\delta_{ij}\beta^2\mathbf{r}_1{}^2+2\beta(1-\beta)(p_{1i}p_{1j}-\beta^2r_{1i}r_{1j})}{(\mathbf{p}_\perp-\beta\mathbf{r}_1)^2+m^2}-\frac{\delta_{ij}(\tfrac{1}{2}-\beta)^2\mathbf{r}_1{}^2+2\beta(1-\beta)[(p_\perp+\frac{1}{2}r_1)_i(p_\perp+\frac{1}{2}r_1)_j-(\frac{1}{2}-\beta)^2r_{1i}r_{1j}]}{[\mathbf{p}_\perp+(1-\beta)\mathbf{r}_1]^2+m^2}\right\}$$
$$\times\left\{\frac{\delta_{i'j'}\beta'^2\mathbf{r}_1{}^2+2\beta'(1-\beta')(p_{1i'}{}'p_{1j'}{}'-\beta'^2r_{1i'}r_{1j'})}{(\mathbf{p}_\perp{}'-\beta'\mathbf{r}_1)^2+m^2}\right.$$
$$\left.-\frac{\delta_{i'j'}(\tfrac{1}{2}-\beta')^2\mathbf{r}_1{}^2+2\beta'(1-\beta')[(p_\perp{}'+\frac{1}{2}r_1)_{i'}(p_\perp{}'+\frac{1}{2}r_1)_{j'}-(\frac{1}{2}-\beta')^2r_{1i'}r_{1j'}]}{[\mathbf{p}_\perp{}'+(1-\beta')\mathbf{r}_1]^2+m^2}\right\}, \tag{4.17}$$

with (4.9) understood.

D. Summary

It is clear from the above examples that for a process $a+b\to a'+b'$, the scattering amplitude in the limit $s\to\infty$, with T fixed, is given by

$$\mathfrak{M}_1^{(ab,a'b')}\sim s^{3/2}\lambda^{-3}J^{aa',bb'}(T), \tag{4.18}$$

where $J^{aa',bb'}(T)$ can be obtained by first writing down $g^{aa'}(\mathbf{r}_1,0)g^{bb'}(\mathbf{r}_1,0)$ in integral form and then multiplying a factor $I(TA^{-1}B^{-1})(AB)^{-1/2}$ to the integrand, where $g^{aa'}(\mathbf{r}_1,\mathbf{q}_1)$ is the impact factor for a to a'. At the threshold $T=0$, we have

$$\mathfrak{M}_1^{(ab,a'b')}\sim\tfrac{1}{8}s^{3/2}(1+i)\lambda^{-3}I^{aa'}I^{bb'}, \tag{4.19}$$

where $I^{aa'}$ can be obtained by first writing down $g^{aa'}(\mathbf{r}_1,0)$ in integral form and then multiplying a factor $A^{-1/2}$ to the integrand. In particular, if a and a' are both the electron, we have

$$I^{ee}=e^2(2m)^{-1}\delta_{12}, \tag{4.20}$$

and if a and a' are both the photon, we have

$$I^{\gamma\gamma}=-\tfrac{1}{2}\pi^{-3}e^4\lambda\int d\mathbf{p}_\perp\int_0^1 d\beta\,\beta^{1/2}(1-\beta)^{1/2}(\mathbf{p}_\perp^2+m^2)^{-1/2}[(\mathbf{p}_\perp+\beta\mathbf{r}_1)^2+m^2]^{-1}$$
$$\times\left\{\frac{\delta_{ij}\beta^2\mathbf{r}_1^2+2\beta(1-\beta)(p_{\perp i}p_{\perp j}-\beta^2r_{1i}r_{1j})}{(\mathbf{p}_\perp-\beta\mathbf{r}_1)^2+m^2}-\frac{\delta_{ij}(\tfrac{1}{2}-\beta)^2\mathbf{r}_1^2+2\beta(1-\beta)[(p_\perp+\tfrac{1}{2}r_1)_i(p_\perp+\tfrac{1}{2}r_1)_j-(\tfrac{1}{2}-\beta)^2r_{1i}r_{1j}]}{[\mathbf{p}_\perp+(1-\beta)\mathbf{r}_1]^2+m^2}\right\}, \tag{4.21}$$

with (4.9) understood.

We note in (4.19) that the coefficient of $s^{3/2}$ for $\mathfrak{M}_1^{(ab,a'b')}$ is *factorized* into a function of a and a' times a function of b and b'. It suggests that the corresponding singularity in the J plane is a Regge pole. We shall study this in more detail in the following sections.

We also emphasize that in the above discussions, a or a' can be multiparticle states. Thus our treatments apply to production processes as well.

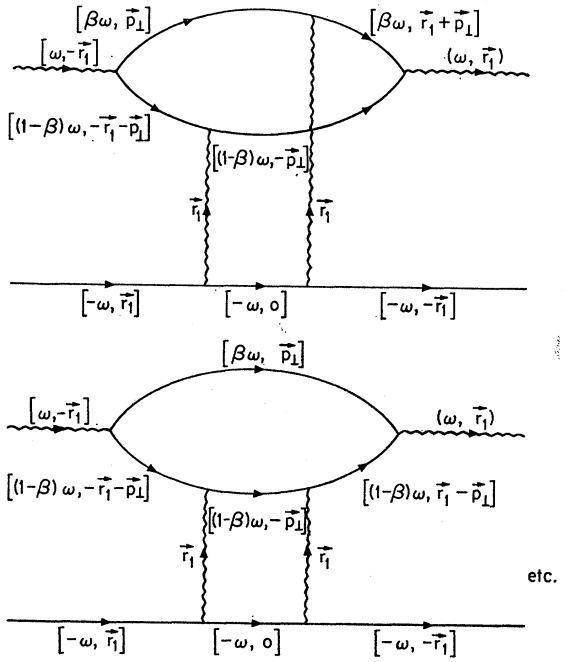

FIG. 4. Lowest-order diagrams for Compton scattering with a two-photon cut in the t channel.

5. TOWER DIAGRAMS

We shall now proceed to examine higher-order diagrams in the limit $s\to\infty$ with T fixed. We shall start with the simplest process of electron-electron scattering. What kind of diagrams shall we consider? There are many higher-order diagrams which give an amplitude satisfying the impact-factor representation when t is away from $4\lambda^2$. They can be handled exactly as in the preceding section, and the amplitude in the limit $s\to\infty$ with T fixed is, in fact, always in the form of (4.19). The lowest-order diagrams which give an amplitude not proportional to s are those illustrated in Fig. 6. They are the lowest-order diagrams for electron-electron scattering with one electron loop. For t away from $4\lambda^2$, the scattering amplitude from the sum of these diagrams gives the amplitude

$$is\ln s(2\pi)^{-4}\int d\mathbf{q}\,d\mathbf{q}_1'\,(g^e)^2K(\mathbf{q}_1,\mathbf{q}_1',\mathbf{r}_1)$$
$$\times[(\mathbf{r}_1+\mathbf{q}_1)^2+\lambda^2]^{-1}[(\mathbf{r}_1-\mathbf{q}_1)^2+\lambda^2]^{-1}$$
$$\times[(\mathbf{r}_1+\mathbf{q}_1')^2+\lambda^2]^{-1}[(\mathbf{r}_1-\mathbf{q}')^2+\lambda^2]^{-1}, \tag{5.1}$$

where $K(\mathbf{q}_1,\mathbf{q}_1',\mathbf{r}_1)$ is given by Eq. (2.14) of Ref. 8. At $t=4\lambda^2$, the integral in (5.1) is again divergent, both at $\mathbf{q}_1=0$ and at $\mathbf{q}_1'=0$. We must apply the rules in Sec. III to take care of this situation.

From Fig. 6 it is clear that we should make the replacement

$$(2\pi)^{-2}\int d\mathbf{q}_1'[(\mathbf{r}_1+\mathbf{q}_1')^2+\lambda^2]^{-1}$$
$$\times[(\mathbf{r}_1-\mathbf{q}_1')^2+\lambda^2]^{-1}\to -is^{1/2}\lambda^{-3}A^{-1/2}I(T/A), \tag{5.2}$$

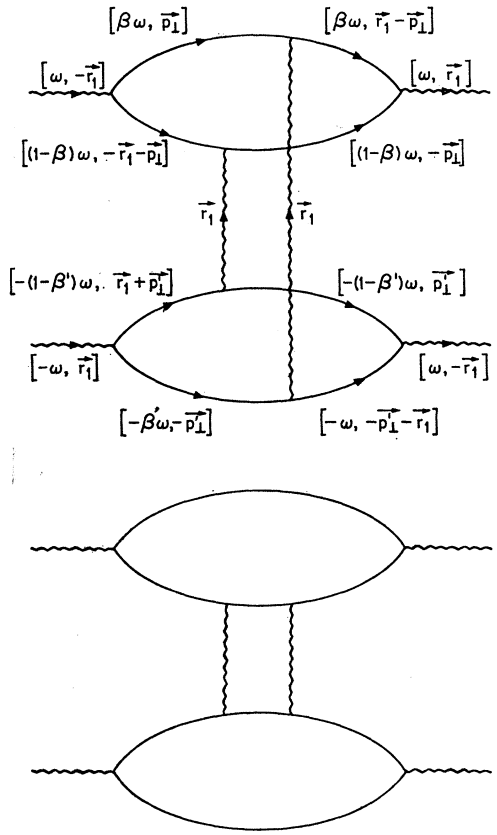

FIG. 5. Lowest-order diagrams for photon-photon scattering with a two-photon cut in the t channel.

where

$$A\sim\lambda^{-2}(\beta_1+\beta_2)\beta_1^{-1}\beta_2^{-1}(\mathbf{p}_\perp^2+m^2). \tag{5.3}$$

In (5.3), we have made the approximations $\beta_1^{-1}\gg 1$, $\beta_2^{-1}\gg 1$, and $|\mathbf{q}_\perp|\ll|\mathbf{p}_\perp|$, which hold in the dominant integration region. Let us put

$$\beta_1=\rho x,\quad \beta_2=\rho(1-x);$$

then

$$A\sim\lambda^{-2}[\rho x(1-x)]^{-1}(\mathbf{p}_\perp^2+m^2). \tag{5.4}$$

Next we must make a replacement for

$$\int d\mathbf{q}_\perp[(\mathbf{r}_1+\mathbf{q}_\perp)^2+\lambda^2]^{-1}[(\mathbf{r}_1-\mathbf{q}_\perp)^2+\lambda^2]^{-1}.$$

We remember that the factor $[(\mathbf{r}_1+\mathbf{q})^2+\lambda^2]^{-1}$ was obtained by approximating the propagation factor

$$[(\mathbf{r}_1+\mathbf{q}_\perp)^2+\lambda^2]/(\beta_1+\beta_2)+(\mathbf{q}_\perp^2+m^2)/(1-\beta_1-\beta_2)-(\mathbf{r}_1^2+m^2) \tag{5.5}$$

by

$$[(\mathbf{r}_1+\mathbf{q}_\perp)^2+\lambda^2]/(\beta_1+\beta_2).$$

This approximation was made with the justification that $\beta_1^{-1}\gg 1$, $\beta_2^{-1}\gg 1$. However, in the present case, this approximation is not valid as $(\mathbf{r}_1+\mathbf{q}_\perp)^2+\lambda^2$ is also very small when $\mathbf{q}_\perp$ is small. Thus in the present case, we must make the following replacement in (5.1):

$$(\mathbf{r}_1\pm\mathbf{q}_\perp)^2+\lambda^2\to(\mathbf{r}_1\pm\mathbf{q}_\perp)^2+\lambda^2+\rho[(\mathbf{q}_\perp^2+m^2)/(1-\beta_1-\beta_2)-(\mathbf{r}_1^2+m^2)]\sim q_2^2\pm 2r_1q_1+\mathbf{r}_1^2+\lambda^2+\lambda^2\rho. \tag{5.6}$$

Finally, we remember that $\ln s$ was obtained from

$$2\int_{\omega^{-1}}^1\rho^{-1}d\rho\sim\ln s. \tag{5.7}$$

Thus ρ is at least of the order of ω^{-1}. For t given by (2.10), we may therefore neglect $\mathbf{r}_1^2+\lambda^2$ in (5.6). Thus we shall make the replacement

$$(2\pi)^{-2}\int d\mathbf{q}_\perp[(\mathbf{r}_1+\mathbf{q}_\perp)^2+\lambda^2]^{-1}\times[(\mathbf{r}_1-\mathbf{q}_\perp)^2+\lambda^2]^{-1}\to(2\pi)^{-2}\int dq_1dq_2\times(q_2^2+2rq_1+\lambda^2\rho)^{-1}(q_2^2-2rq_1+\lambda^2\rho)^{-1}=\tfrac{1}{8}\lambda^{-2}\rho^{-1/2}. \tag{5.8}$$

From (5.1), (5.2), (5.4), (5.8), and Eq. (2.14) of Ref. 8, we get

$$\mathfrak{M}_2^{(--)}\sim\tfrac{1}{8}(1+i)s^{3/2}\ln s\,\lambda^{-3}(g^e)^2\kappa, \tag{5.9}$$

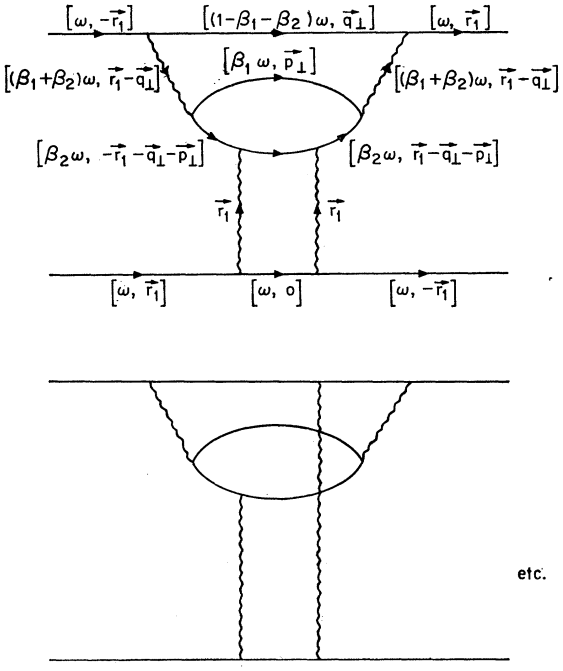

FIG. 6. Eighth-order tower diagrams for electron-electron scattering.

where

$$\kappa=\tfrac{1}{2}(2\pi)^{-4}\lambda^{-1}e^4\int d\mathbf{p}_\perp\int_0^1 dx\,[x(1-x)]^{1/2}(\mathbf{p}_\perp^2+m^2)^{-1/2}[\mathbf{p}_\perp^2+m^2-x\lambda^2+2x\mathbf{r}_1\cdot\mathbf{p}_\perp]^{-1}$$
$$\times\left\{\frac{(\mathbf{p}_\perp^2+m^2)(\mathbf{p}_\perp^2+\lambda^2+m^2)}{\mathbf{p}_\perp^2+m^2-x\lambda^2-2x\mathbf{r}_1\cdot\mathbf{p}_\perp}-\frac{(\mathbf{p}_\perp^2+m^2)(\mathbf{p}_\perp^2+\lambda^2+m^2)+2(\mathbf{p}_\perp\cdot\mathbf{r}_1)^2+2(\mathbf{p}_\perp^2+m^2)\mathbf{p}_\perp\cdot\mathbf{r}_1}{\mathbf{p}_\perp^2+m^2-(1-x)\lambda^2+2(1-x)\mathbf{r}_1\cdot\mathbf{p}_\perp}\right\},\quad(5.10)$$

with $\mathbf{r}_1^2=-\lambda^2$. Notice that $\mathfrak{M}_2^{(--)}$ is independent of T. In Appendix B we shall show that κ is positive if $\lambda^2\leq m^2$.[17]

Next we consider the n-loop diagrams illustrated in Fig. 1. Repeating the same arguments as above, we easily get

$$\mathfrak{M}_{n+1}^{(--)}\sim\tfrac{1}{8}(1+i)[s^{3/2}(\ln s)^n/n!]\lambda^{-3}(g^e)^2\kappa^n\quad(5.11)$$

and

$$\mathfrak{M}^{(--)}=\sum_{n=0}^{\infty}\mathfrak{M}_{n+1}^{(--)}=\tfrac{1}{8}(1+i)\lambda^{-3}(g^e)^2s^{3/2+\kappa}.\quad(5.12)$$

Extension of the treatments above to a general process $a+b\to a'+b'$ is also trivial. We get

$$\mathfrak{M}^{(ab,a'b')}\sim\tfrac{1}{8}(1+i)\lambda^{-3}I^{aa'}I^{bb'}s^{3/2+\kappa}.\quad(5.13)$$

Equation (5.13) shows that the leading singularity in the J plane for $t\sim4\lambda^2$ is a moving Regge pole with factorizable residues.

6. DISCUSSION

We discuss the significance of (5.13). Equation (5.13) shows that when t is near $4\lambda^2$, the leading singularity in the J plane comes from the tower diagrams and is a *moving Regge pole* located to the right of $J=\frac{3}{2}$. Our previous calculations indicate that for $t\leq0$, the leading singularities in the J plane are *branch points* with $\mathrm{Re}J=1$. These branch points start to move when t is positive,[18] and for some t between 0 and $4\lambda^2$, a Regge pole emerges from the second sheet through one branch point and moves ahead. At $t=4\lambda^2$, this Regge pole is in the neighborhood of $J=\frac{3}{2}$ if the coupling is weak, and is further to the right for strong couplings. This is schematically plotted in Fig. 7.

Gribov[19] argued that the scattering amplitude cannot be of the form $sf(t)$ when t is above the elastic threshold. Apparently, the promotion phenomenon guarantees the scattering amplitude to be at least of the order of $s^{3/2}$ at $t=4\lambda^2$. Thus Gribov's paradox is trivially resolved.

Promotion always occurs when t is at a two-body threshold. What we have found here is a diagrammatic way to study the promotion. For instance, our argument shows that the diagrams which generate the fermion Regge pole[20] are promoted from $s^{1/2}$ to s at $t=(M+\lambda)^2$, where M is the mass of the fermion. Thus the fermion pole is in the neighborhood of $J=1$ at $t=(M+\lambda)^2$. On the other hand, no promotion occurs on a three-particle threshold.

[17] We must remember that we are studying the scattering amplitude at $t\sim4\lambda^2$. If $\lambda^2>m^2$, then $4\lambda^2$ already exceeds the lowest threshold and κ is complex.

[18] A detailed discussion of this point will be contained in H. Cheng and T. T. Wu, Phys. Rev. (to be published).

[19] V. N. Gribov, Nucl. Phys. **22**, 249 (1961).

ACKNOWLEDGMENT

We are greatly indebted to Professor C. N. Yang for most helpful discussions.

APPENDIX A

In this appendix we derive (3.13) from (3.12).

Let us take the x axis to be in the direction of $\mathbf{r}_{1\perp}$ and denote $\mathbf{r}_{1\perp}=r_{1\perp}\mathbf{e}_x$, $\mathbf{q}_\perp=q_1\mathbf{e}_x+q_2\mathbf{e}_y$. We shall make the approximation

$$[(r_1+q)^2-\lambda^2+i\epsilon][(r_1-q)^2-\lambda^2+i\epsilon]$$
$$\sim[(r_1+q)_+(r_1+q)_--\mathbf{r}_{1\perp}^2-\lambda^2-q_2^2-2r_{1\perp}q_1+i\epsilon]$$
$$\times[(r_1-q)_+(r_1-q)_--\mathbf{r}_{1\perp}^2-\lambda^2-q_2^2+2\mathbf{r}_{1\perp}q_1+i\epsilon].\quad(A1)$$

In both of the factors in (A1), a term q_1^2 has been neglected since q_1 is of the order of s^{-1}. Thus carrying

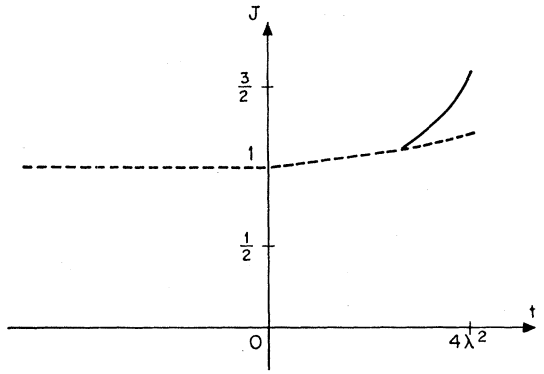

FIG. 7. Schematic plot for the Pomeranchuk singularity. The dotted line represents the position of the real part of the branch point, and the solid line represents the position of the Regge pole.

[20] M. Gell-Mann, M. L. Goldberger, F. E. Low, E. Marx, and F. Zachariasen, Phys. Rev. **133**, B145 (1964); H. Cheng and T. T. Wu, *ibid.* **140**, B465 (1965).

out the integration over q_1 and q_2 successively, we get

$$\int dq_1[(r_1+q)^2-\lambda^2+i\epsilon]^{-1}[(r_1-q)^2-\lambda^2+i\epsilon]$$

$$\sim\tfrac{1}{2}\pi i(r_{11})^{-1}\int dq_2[-q_+q_--\tfrac{1}{4}t+\lambda^2+q_2^2-i\epsilon]^{-1}$$

$$=\tfrac{1}{2}\pi i(r_{11})^{-1}[-q_+q_--\tfrac{1}{4}t+\lambda^2-i\epsilon]^{-1/2}$$

$$\sim-\tfrac{1}{2}\pi^2\lambda^{-1}[-q_+q_-+\lambda^4T/s-i\epsilon]^{-1/2}. \quad \text{(A2)}$$

The left-hand side of (3.12) is therefore approximately equal to

$$\tfrac{1}{8}(2\pi)^{-2}\lambda^3\omega^{-2}AB\int dq_+dq_-[-q_+q_-+\lambda^4T/s-i\epsilon]^{-1/2}$$

$$\times[\lambda^4(A-i\epsilon)^2/s-q_-^2]^{-1}[\lambda^4(B-i\epsilon)^2/s-q_+^2]. \quad \text{(A3)}$$

Putting

$$q_+=\lambda^2Bs^{-1/2}u \quad \text{(A4)}$$

and

$$q_-=\lambda^2As^{-1/2}v, \quad \text{(A5)}$$

we reduce (A3) to the right-hand side of (3.12):

$$-i\lambda^{-3}s^{1/2}(AB)^{-1/2}I(TA^{-1}B^{-1}),$$

with

$$I(x)=\tfrac{1}{2}i(2\pi)^{-2}\int_{-\infty}^{\infty}dudv\,[-uv+x-i\epsilon]^{-1/2}$$

$$\times(1-u^2-i\epsilon)^{-1}(1-v^2-i\epsilon)^{-1}. \quad \text{(A6)}$$

Equation (A6) gives (3.13) after standard integrations.

APPENDIX B

In this appendix we shall show that κ is positive, if $\lambda\leq m$.

From (5.10), we have

$$\kappa=\tfrac{1}{2}(2\pi)^{-4}\lambda^{-1}e^4\int d\mathbf{p}_\perp\int_0^1 dx\,[x(1-x)]^{1/2}(\mathbf{p}_\perp^2+m^2)^{-1/2}$$

$$\times\frac{N(\mathbf{p}_\perp)}{(\mathbf{p}_\perp^2+m^2-x\lambda^2+2x\mathbf{r}_1\cdot\mathbf{p}_\perp)(\mathbf{p}_\perp^2+m^2-x\lambda^2-2x\mathbf{r}_1\cdot\mathbf{p}_\perp)[\mathbf{p}_\perp^2+m^2-(1-x)\lambda^2+2(1-x)\mathbf{r}_1\cdot\mathbf{p}_\perp]}, \quad \text{(B1)}$$

where

$$N(p_\perp)=(\mathbf{p}_\perp^2+m^2)(\mathbf{p}_\perp^2+\lambda^2+m^2)[\mathbf{p}_\perp^2+m^2-(1-x)\lambda^2+2(1-x)\mathbf{r}_1\cdot\mathbf{p}_\perp]$$

$$-[(\mathbf{p}_\perp^2+m^2)(\mathbf{p}_\perp^2+\lambda^2+m^2)+2(\mathbf{p}_\perp\cdot\mathbf{r}_1)^2+2(\mathbf{p}_\perp^2+m^2)(\mathbf{p}_\perp\cdot\mathbf{r}_1)](\mathbf{p}_\perp^2+m^2-x\lambda^2-2x\mathbf{r}_1\cdot\mathbf{p}_\perp)$$

$$=-(\mathbf{p}_\perp^2+m^2)(\mathbf{p}_\perp^2+m^2+\lambda^2)\lambda^2(1-2x)+2\mathbf{r}_1\cdot\mathbf{p}_\perp(\mathbf{p}_\perp^2+m^2)\lambda^2(1+x)$$

$$-2(\mathbf{r}_1\cdot\mathbf{p}_\perp)^2[(1-2x)(\mathbf{p}_\perp^2+m^2)-x\lambda^2-2x\mathbf{r}_1\cdot\mathbf{p}_\perp]. \quad \text{(B2)}$$

Since an odd function of $\mathbf{p}_\perp$ in the integrand of (B1) is integrated to zero, we can symmetrize the integrand of (B1) to obtain

$$\kappa=\tfrac{1}{2}(2\pi)^{-4}\lambda^{-1}e^4\int d\mathbf{p}_\perp\int_0^1 dx\,[x(1-x)]^{1/2}(\mathbf{p}_\perp^2+m^2)^{-1/2}$$

$$\times\frac{\mathfrak{N}}{[(\mathbf{p}_\perp^2+m^2-x\lambda^2)^2+4x^2\lambda^2p_1^2]\{[\mathbf{p}_\perp^2+m^2-(1-x)\lambda^2]^2+4(1-x)^2\lambda^2p_1^2\}}, \quad \text{(B3)}$$

where p_1 is the component of $\mathbf{p}_\perp$ in the direction of $\mathbf{r}_1$, and where

$$\mathfrak{N}=\tfrac{1}{2}N(\mathbf{p}_\perp)[\mathbf{p}_\perp^2+m^2-(1-x)\lambda^2-2(1-x)\mathbf{r}_1\cdot\mathbf{p}_\perp]$$

$$+\tfrac{1}{2}N(-\mathbf{p}_\perp)[\mathbf{p}_\perp^2+m^2-(1-x)\lambda^2+2(1-x)\mathbf{r}_1\cdot\mathbf{p}_\perp]$$

$$=-(\mathbf{p}_\perp^2+m^2)(\mathbf{p}_\perp^2+m^2+\lambda^2)\lambda^2(1-2x)$$

$$\times[\mathbf{p}_\perp^2+m^2-(1-x)\lambda^2]$$

$$+2\lambda^2p_1^2[(1-2x)(\mathbf{p}_\perp^2+m^2)-x\lambda^2]$$

$$\times[\mathbf{p}_\perp^2+m^2-(1-x)\lambda^2]$$

$$+4\lambda^4p_1^2(\mathbf{p}_\perp^2+m^2)(1-x^2)-8x(1-x)\lambda^4p_1^4. \quad \text{(B4)}$$

Since all factors except $\mathfrak{N}$ in the integrand of (B3) are symmetrical with respect to $x\leftrightarrow(1-x)$, $\mathfrak{N}$ is further reduced to

$$\mathfrak{N}=2(\tfrac{1}{2}-x)^2(\mathbf{p}_\perp^2+m^2)(\mathbf{p}_\perp^2+m^2+\lambda^2)\lambda^4$$

$$-4(\tfrac{1}{2}-x)^2p_1^2(\mathbf{p}_\perp^2+m^2)\lambda^4-\lambda^4p_1^2(\mathbf{p}_\perp^2+m^2)$$

$$+2x(1-x)\lambda^6p_1^2+4\lambda^4p_1^2(\mathbf{p}_\perp^2+m^2)$$

$$\times(1-x^2)-8x(1-x)\lambda^4p_1^4$$

$$=2(\tfrac{1}{2}-x)^2(\mathbf{p}_\perp^2+m^2)(\mathbf{p}_\perp^2+m^2+\lambda^2)\lambda^4$$

$$+8x(1-x)p_1^2(p_2^2+m^2)\lambda^4+2x(1-x)p_1^2\lambda^6, \quad \text{(B5)}$$

where p_2 is the component of $\mathbf{p}_\perp$ in the direction perpendicular to $\mathbf{r}_1$. From (B3) and (B5), we see that κ is greater than zero. Note that, if $\lambda>m$, the integral (B3) is divergent at $p_1=0$ and $x=(m^2+p_2^2)/\lambda^2$ as well as at $p_1=0$ and $1-x=(m^2+p_2^2)/\lambda^2$, in the region $p_2^2<\lambda^2-m^2$. Thus κ must be defined by analytic continuation of $\lambda^2>m^2$.